Palaeogeography, Palaeoclimatology, Palaeoecology 350–352 (2012) 236–246

Contents lists available at SciVerse ScienceDirect

Palaeogeography, Palaeoclimatology, Palaeoecology

journal homepage: www.elsevier.com/locate/palaeo

# Marine climatic seasonality during medieval times (10th to 12th centuries) based on isotopic records in Viking Age shells from Orkney, Scotland

Donna Surge [a,*], James H. Barrett [b]

[a] University of North Carolina, Department of Geological Sciences, 104 South Road, CB #3315, Chapel Hill, North Carolina, USA
[b] McDonald Institute for Archaeological Research, University of Cambridge, Downing Street, Cambridge, CB2 3ER, UK

ARTICLE INFO

*Article history:*
Received 1 March 2012
Received in revised form 2 July 2012
Accepted 8 July 2012
Available online 16 July 2012

*Keywords:*
Medieval Warm Period
Oxygen isotope ratios
*Patella vulgata*
Late Holocene
Quoygrew
Sea surface temperature

ABSTRACT

Seasonal sea-surface temperature (SST) variability during the Medieval Climate Anomaly (MCA), which corresponds to the height of Viking exploration (800–1200 AD), was estimated using oxygen isotope ratios ($\delta^{18}O$) obtained from high-resolution samples micromilled from archaeological shells of the European limpet, *Patella vulgata*. Our findings illustrate the advantage of targeting SST archives from fast-growing, short-lived molluscs that capture summer and winter seasons simultaneously. Shells from the 10th to 12th centuries (early MCA) were collected from well-stratified horizons, which accumulated in Viking shell and fish middens at Quoygrew on Westray in the archipelago of Orkney, Scotland. Their ages were constrained based on artifacts and radiocarbon dating of bone, charred cereal grain, and the shells used in this study. We used measured $\delta^{18}O_{WATER}$ values taken from nearby Rack Wick Bay (average $0.31 \pm 0.17$‰ VSMOW, $n = 11$) to estimate SST from $\delta^{18}O_{SHELL}$ values. The standard deviation of $\delta^{18}O_{WATER}$ values resulted in an error in SST estimates of $\pm 0.7$ °C. The coldest winter months recorded in the shells averaged $6.0 \pm 0.6$ °C and the warmest summer months averaged $14.1 \pm 0.7$ °C. Winter and summer SST during the late 20th century (1961–1990) was $7.77 \pm 0.40$ °C and $12.42 \pm 0.41$ °C, respectively. Thus, during the 10th to 12th centuries winters were colder and summers were warmer by ~2 °C and seasonality was higher relative to the late 20th century. Without the benefit of seasonal resolution, SST averaged from shell time series would be weighted toward the fast-growing summer season, resulting in the conclusion that the early MCA was warmer than the late 20th century by ~1 °C. This conclusion is broadly true for the summer season, but not true for the winter season. Higher seasonality and cooler winters during early medieval times may result from a weakened North Atlantic Oscillation index.



## 1. Introduction

Late Holocene climate episodes provide critical information about pre-industrial climate change relevant to understanding natural variation in the climate system. Recent attention has focused on temporal and spatial variability during the Medieval Climate Anomaly (MCA) and Little Ice Age (LIA) (Jansen et al., 2007; Mann et al., 2009; Trouet et al., 2009; Diaz et al., 2011; Graham et al., 2011). Graham et al. (2011) and Diaz et al. (2011) provide an excellent historical background and synthesis of proxy records, regional climate reconstructions, and results from climate model experiments supporting global climate reorganization during the MCA and LIA. This interval of time is significant culturally because it spans the height of Viking (Scandinavian) exploration and economic intensification during the MCA (800–1200 AD), and subsequent retrenchment in the early LIA (1200–1550 AD). Paleoclimate reconstructions that use archaeological sources contribute to our understanding of human–climate interactions (Surge and Walker, 2005; Walker and Surge, 2006; Hallmann et al., 2009; Hufthammer et al., 2010; Jones et al., 2010; Andrus, 2011; Helama and Hood, 2011; Wang et al., 2011, 2012), especially in regions that are sensitive to climate change.

Proxy records reconstructing climatic conditions during the MCA are strongly biased towards decadal to annual resolution and summer/growing seasons (e.g., Table 6.1 in Jansen et al., 2007 and Table 1 in Christiansen and Ljungqvist, 2011). Few studies resolve the winter season. Those that do focus on winter precipitation and even fewer report on winter air temperatures, which are reconstructed based on documentary evidence (Ogilvie and Farmer, 1997; Pfister et al., 1998). Studies of pre-industrial climate change that resolve summer and winter variability in sea surface temperature (SST) are scarce (Patterson et al., 2010; Wanamaker et al., 2011). Regional climate models illustrate the need for such high-resolution studies at seasonal time scales. Numerical (idealized multi-level primitive equation) and sensitivity (ECBilt-Clio) model experiments demonstrate that small changes in the coupled atmospheric-oceanographic climate system influence regional mid-latitude seasonality (Lee and Kim, 2003; van der Schrier et al., 2007). These model simulations for the North Atlantic sector show that minute changes in the position and intensity of the subtropical jet stream at low latitudes restrict the polar front jet stream

* Corresponding author. Tel.: +1 919 843 1994; fax: +1 919 966 4519.
*E-mail addresses:* donna64@unc.edu (D. Surge), jhb41@cam.ac.uk (J.H. Barrett).

0031-0182/$ – see front matter © 2012 Elsevier B.V. All rights reserved.
doi:10.1016/j.palaeo.2012.07.003

**Table 1**
Time range of the archaeological limpet shells.

| Specimen no. | NOSAMS no. | AMS radiocarbon age, $^{14}$C cal BP | $\delta^{13}$C (VPDB ‰) | 2 Sigma calibration |
|---|---|---|---|---|
| QG2-7180-1 | OS-95722 | 1250 ± 25 | 0.39 | cal BP 721–979 (cal AD 971–1229) |
| QG2-7180-2 | OS-95723 | 1250 ± 25 | 2.13 | cal BP 721–979 (cal AD 971–1229) |
| QG2-1064-1 | OS-95724 | 1260 ± 20 | 0.59 | cal BP 730–988 (cal AD 962–1220) |
| QG2-1061-1 | OS-95725 | 1270 ± 20 | 1.54 | cal BP 739–1005 (cal AD 945–1211) |
| QG1-7246-1 | OS-95727 | 1350 ± 30 | −0.39 | cal BP 822–1122 (cal AD 828–1128) |
| QG1-7189-2 | OS-95726 | 1370 ± 20 | 1.68 | cal BP 876–1140 (cal AD 810–1074) |
| QG1-7188-1 | OS-95728 | 1390 ± 25 | 1.10 | cal BP 896–1156 (cal AD 794–1054) |

to high latitudes. As with a positive North Atlantic Oscillation (NAO) index (a stronger than usual subtropical high pressure center and a deeper than usual Icelandic low), restriction of the polar front jet stream to high latitudes (i.e., a decrease in atmospheric meridional heat transport) and an intensified Gulf Stream (i.e., an increase in oceanic meridional heat transport) transfers a broad band of moisture and latent heat farther northeast. Simulations of the enhanced meridional heat transport as a result of these complementary atmospheric–oceanic processes generate equable climate at mid latitudes and demonstrate the potential sensitivity of mid-latitude regions to seasonal-scale changes.

Archives from fast-growing shells can potentially capture summer and winter seasons and, thus, approach the full seasonal range of sea surface temperature (SST). Often, fast-growing shells are short-lived and, thus, provide "snapshots" of multi-year seasonal cycles. Archaeological limpet shells of the genus, *Patella*, collected by the local human inhabitants are potentially valuable archives of variability in seasonal SST from coastal marine environments (Shackleton, 1973; Cohen and Branch, 1992; Fenger et al., 2007; Ferguson et al., 2011; Wang et al., 2012). This study presents reconstructed mid-latitude SST at seasonal time scales using oxygen isotope ($\delta^{18}$O) proxy data from shells of the European limpet, *P. vulgata*, harvested by the inhabitants of the Quoygrew archaeological site on Westray in the archipelago of Orkney (a Scandinavian colony of the Viking Age that came under Scottish rule in 1468 AD) (Fig. 1). We tested the hypothesis that seasonal variability in coastal SST during the 10th to 12th centuries was similar to that of the late 20th century (1960–1991).

## 2. Study area

### 2.1. Archaeological context

The Quoygrew archaeological site (59.34°N, 2.98°W) is located at the head of Rack Wick Bay on the island of Westray in the archipelago of Orkney, north of mainland Scotland (Fig. 1). It was a rural farming and fishing settlement occupied between the 10th century AD and 1937. Excavation focused on houses and associated middens (refuse dumps) dating from the earliest seven centuries of this millennium-long sequence. Midden deposits from the 10th to 15th centuries (MCA-LIA) were particularly well stratified. For the present study we focus on shells from layers radiocarbon dated to the 10th century (Phase 1) and to the 11th to 12th centuries (Phase 2). The Phase 1 specimens derive from early midden strata of the so-called farm mound, a build-up of superimposed household refuse, discarded animal bedding, fuel residues and demolished buildings approximately 50 m from the shoreline. The Phase 2 specimens derive from strata higher in the same farm mound (QG2-7180-1, and QG2-7180-2) and from the basal layers of a semi-specialized fish processing midden at the wave-cut bank (QG2-1061-1, QG2-1064-1) (Barrett, 2005, in press; Simpson et al., 2005). Limpets were the most common molluscs represented in the fish midden and farm mound at Quoygrew. Their abundant shells probably represent the collection of bait for fishing, although some limpets may also have been eaten by the site's inhabitants (Milner et al., 2007).

### 2.2. Oceanographic setting

Physical and chemical oceanographic features of continental slope and shelf waters along western Scotland have been well studied since the 1980s (Inall et al., 2009 and references therein). Offshore, the northward flowing European Slope Current acts as an effective barrier to lateral exchange between coastal shelf and deep ocean waters (Huthnance, 1992, 1995), although Souza et al. (2001) have observed winter intrusions of European Slope Current water onto the shelf.

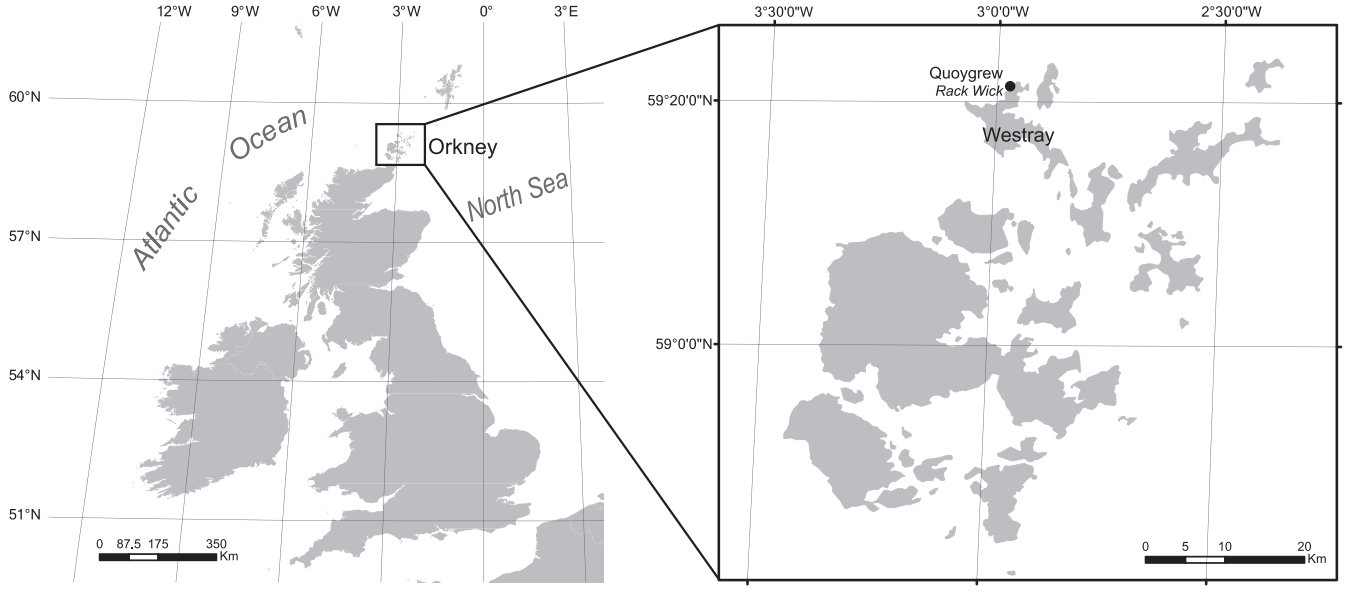


**Fig. 1.** Map of Scotland and Orkney locating the Quoygrew archaeological site on Westray and Rack Wick Bay.

Along the coastline, the Scottish Coastal Current flows northward and carries a mixture of marine water from the Irish and Clyde Seas. Although some coastal regions of western Scotland are influenced by freshwater input from fjords which can slightly dilute the Scottish Coastal Current, the North Atlantic coast of Orkney is dominated by well-mixed shelf water (Connor et al., 2006). In the first systematic review of long-term averaged modern spatial and temporal patterns of $\delta^{18}O_{SEAWATER}$ values from the shelf seas around NW Europe, Austin et al. (2006) report that the seasonal changes in the salinity:$\delta^{18}O_{WATER}$ relationship over most of the NW European shelf can largely be ignored. At normal marine salinities, seasonal changes in the freshwater (i.e., meteoric) end member are unlikely to produce a major signal in the oxygen isotope ratio of seawater. Moreover, the European coastal waters least likely to be affected by changes in salinity:$\delta^{18}O_{WATER}$ relationships are those to the west where the freshwater end member is least depleted in $^{18}O$ (Austin and Inall, 2002; Owen et al., 2002; Scourse et al., 2004). The following mixing equation reported by Austin and Inall (2002) and Austin et al. (2006) best characterizes the salinity:$\delta^{18}O_{WATER}$ relationship for our study area:

$$\delta^{18}O_{WATER} = 0.18^{*}S - 6.0 \quad (1)$$

where S is salinity in psu (practical salinity units).

Since 1975, the Scottish Association for Marine Science has maintained water monitoring stations on the northwest European Continental Shelf off the west coast of Scotland. Inall et al. (2009) analyzed the time series and provided an excellent overview of the regional hydrography. Salinity is relatively invariant across the time series, ranging from 34.0 to 34.5 psu. Given mixing Eq. (1), estimated $\delta^{18}O_{WATER}$ for that salinity range is between 0.12‰ and 0.21‰ (Vienna Standard Mean Ocean Water; VSMOW). SST shows a strong seasonal component and an overall warming trend of +0.57 °C per decade since the late 1980s. The seasonal SST cycle of nearshore coastal waters has a higher amplitude relative to outer shelf water, and coastal waters are more closely coupled to atmospheric thermal forcing relative to offshore waters. Observed multidecadal variability in SST and flow velocity of the Scottish Coastal Current is likely related to fluctuations in the NAO phase, and climatically driven circulation changes link Scottish coastal regions to the North Atlantic (Holliday, 2003).

## 3. Materials and methods

### 3.1. Water sampling and oxygen isotope analysis

Monthly water samples for $\delta^{18}O$ analysis were collected from the large northwest-facing bay, Rack Wick, on Westray, Orkney (Fig. 1). Fifteen milliliters of water were collected once a month from August 2005 to 2006 (missing months December 2005 and June 2006, n = 11). Salinity was measured using a refractometer with an accuracy of 0.5 psu. Water samples were analyzed on a Finnigan Delta-S dual inlet mass spectrometer using an automated $CO_2$–$H_2O$ equilibration unit. Standardization is based on internal standards referenced to VSMOW and VSLAP (Vienna Standard Light Antarctic Precipitation). Precision is better than ±0.08‰ and $\delta^{18}O_{WATER}$ values are reported relative to the VSMOW standard.

### 3.2. Shell selection and sampling

*P. vulgata* shells were selected from the earlier archaeological field campaign at Quoygrew, which were archived at the Orkney Museum in Kirkwall. Three shells were selected from Phase 1 (c. 10th century; specimens QG1-7188-1, QG1-7189-2, and QG1-7246-1) and four shells were selected from Phase 2 (c. 11th–12th centuries; specimens QG2-1061-1, QG2-1064-1, QG2-7180-1, and QG2-7180-2) (Fig. 2). The selected shells were dated by accelerator mass spectrometry (AMS) at the National Ocean Sciences AMS Facility, Woods Hole Oceanographic Institution. Radiocarbon dates of the archaeological shells were calibrated using MARINE09 of CALIB 6.0 (Hughen et al., 2004; Reimer et al., 2009) and corrected for the global ocean reservoir effect (408 years), local reservoir effect (−69 ± 53 years; Russell et al., 2011), and $^{13}C$ fractionation (Stuiver et al., 2005) (Table 1). The selected shells were cut along the maximum axis of growth (anterior to posterior) using a Gryphon diamond band saw, and thick sections made using a Beuhler Isomet low-speed saw. Cross-sections were polished down to 1 μm diamond suspension grit using a Beuhler MetaServ 2000 variable speed grinder-polisher. Because of their fast growth rate, shells were microsampled along the outer, concentric cross-foliated and radial, cross-foliated calcite layers (see Fig. 3 in Fenger et al., 2007) at monthly to fortnightly resolution where annual growth was >1 mm (25 ± 9 samples per year; ~20–50 μg per sample). Microsampling was performed using a New Wave/Merchantek microsampling system fashioned with a Beuhler carbide dental scriber (part number H1621.11.008). Specimen QG1-7246-1 was sampled at lower resolution (7 ± 2 samples/year) because of closely spaced annual growth lines (<1 mm). Annual growth lines determined by sclerochronologic analysis guided our sampling strategy (Fig. 2).

### 3.3. Isotopic analysis of shells and growth temperature calculation

Oxygen isotope ratios of carbonate powdered samples were measured using an automated carbonate preparation device (Kiel-III) coupled to a gas-ratio mass spectrometer (Finnigan MAT 252). Powdered samples were reacted with dehydrated phosphoric acid under vacuum at 70 °C for 1 h. Isotope ratios were calibrated based on repeated measurements of NBS-19 (National Bureau of Standard) and NBS-18. The precision of the measurement was ±0.1‰ for $\delta^{18}O$ (1σ). The results are reported in per mil units (‰) relative to the VPDB (Vienna Pee Dee Belemnite) standard.

We estimated temperature from $\delta^{18}O_{SHELL}$ values using the equilibrium fractionation equation for calcite and water (Friedman and O'Neil, 1977, modified from Tarutani et al., 1969),

$$1000\ln\alpha = 2.78 \times 10^{6}/T^{2} - 2.89 \quad (2)$$

where T is temperature in Kelvin and α is the fractionation factor between calcite and water. Following the procedures described in Fenger, et al. (2007) for *P. vulgata*, we subtracted 1.01‰ from $\delta^{18}O_{SHELL}$ values to account for the predictable positive offset from equilibrium values. The relationship between α and δ is

$$\alpha = (\delta_{SHELL} + 1000)/(\delta_{WATER} + 1000) \quad (3)$$

where δ is expressed relative to VSMOW. Based on our collected water samples, we used a $\delta^{18}O_{WATER}$ value of 0.31 ± 0.17‰ (VSMOW) (n = 11; Table 2). The standard deviation associated with the water measurements resulted in an error in temperature estimates of ±0.7 °C. $\delta^{18}O_{SHELL}$ values were converted from the VPDB to the VSMOW scale using the following equation reported by Coplen et al. (1983) and Gonfiantini et al. (1995):

$$\delta^{18}O_{(VSMOW)} = 1.03091\delta^{18}O_{(VPDB)} + 30.91 \quad (4)$$

## 4. Results

### 4.1. Salinity and oxygen isotope ratios of water

Salinity of monthly water samples taken at Rack Wick Bay collected from August 1, 2005 to August 24, 2006 is relatively stable, averaging 34.8 ± 0.5 psu (n = 11) and ranging from 34.0 to 35.5 psu (Table 2). Oxygen isotope ratios also have minimal variability

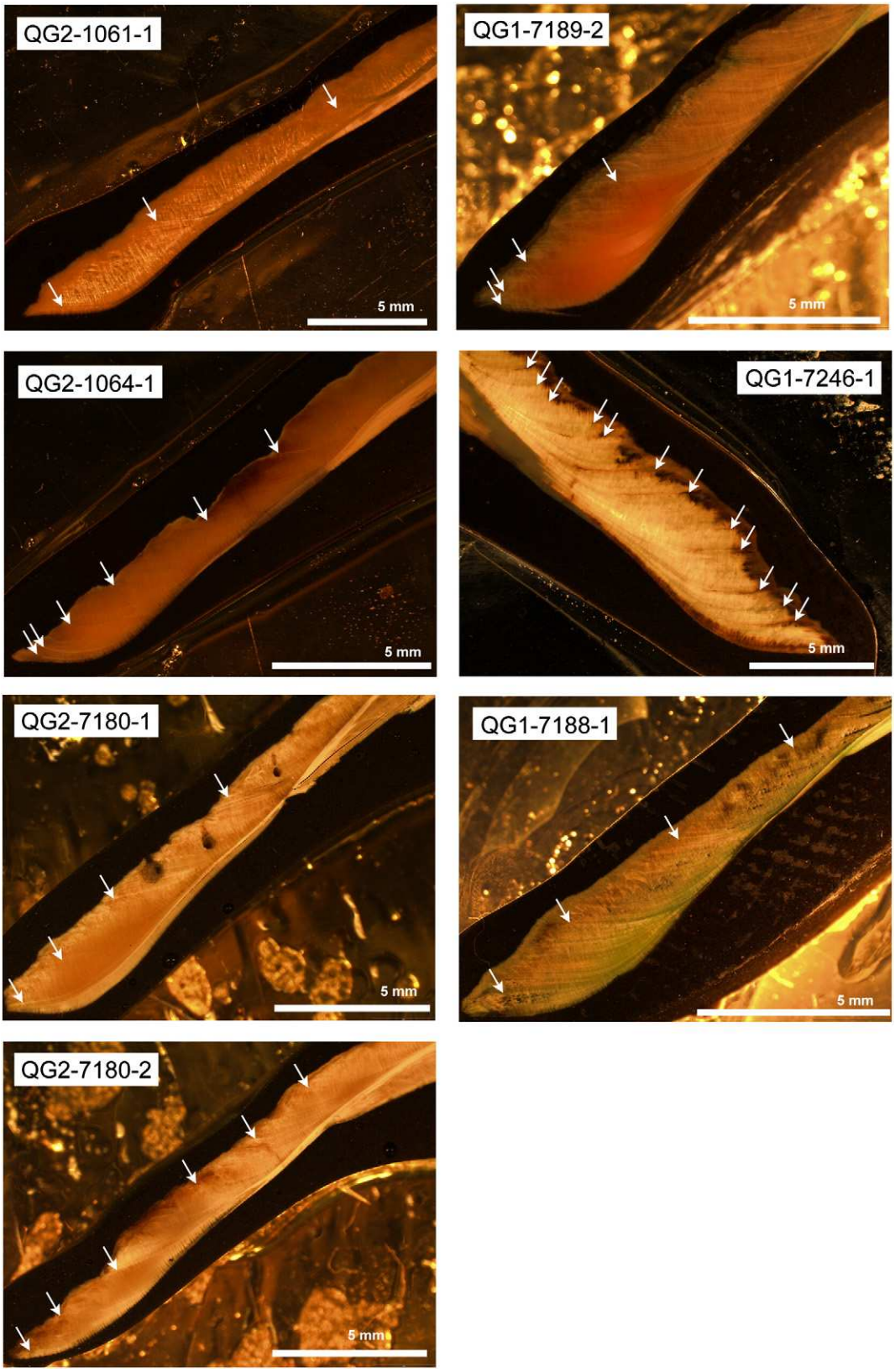


**Fig. 2.** Cross-section along the axis of maximum growth of archaeological shells from Phase 1 (QG1 specimens; 10th century) and Phase 2 (QG2 specimens; 11th–12th centuries). Arrows point to prominent growth lines. White bar is 5 mm.

(Table 2). Measured values average 0.31 ± 0.17‰ (VSMOW; n = 11) and range from −0.12‰ to 0.45‰. Samples taken during year 2006 are especially invariant, averaging +0.40 ± 0.04‰ (n = 7). Estimated values based on mixing Eq. (1) are consistent with measured values, averaging 0.27 ± 0.09‰ and ranging from 0.12‰ to 0.39‰ (Table 2). The measured salinity and $\delta^{18}O_{WATER}$ data sets exhibit no seasonal variability despite the negative excursion in $\delta^{18}O$ values taken in November 2005. The negative excursion in $\delta^{18}O$ values is an outlier that does

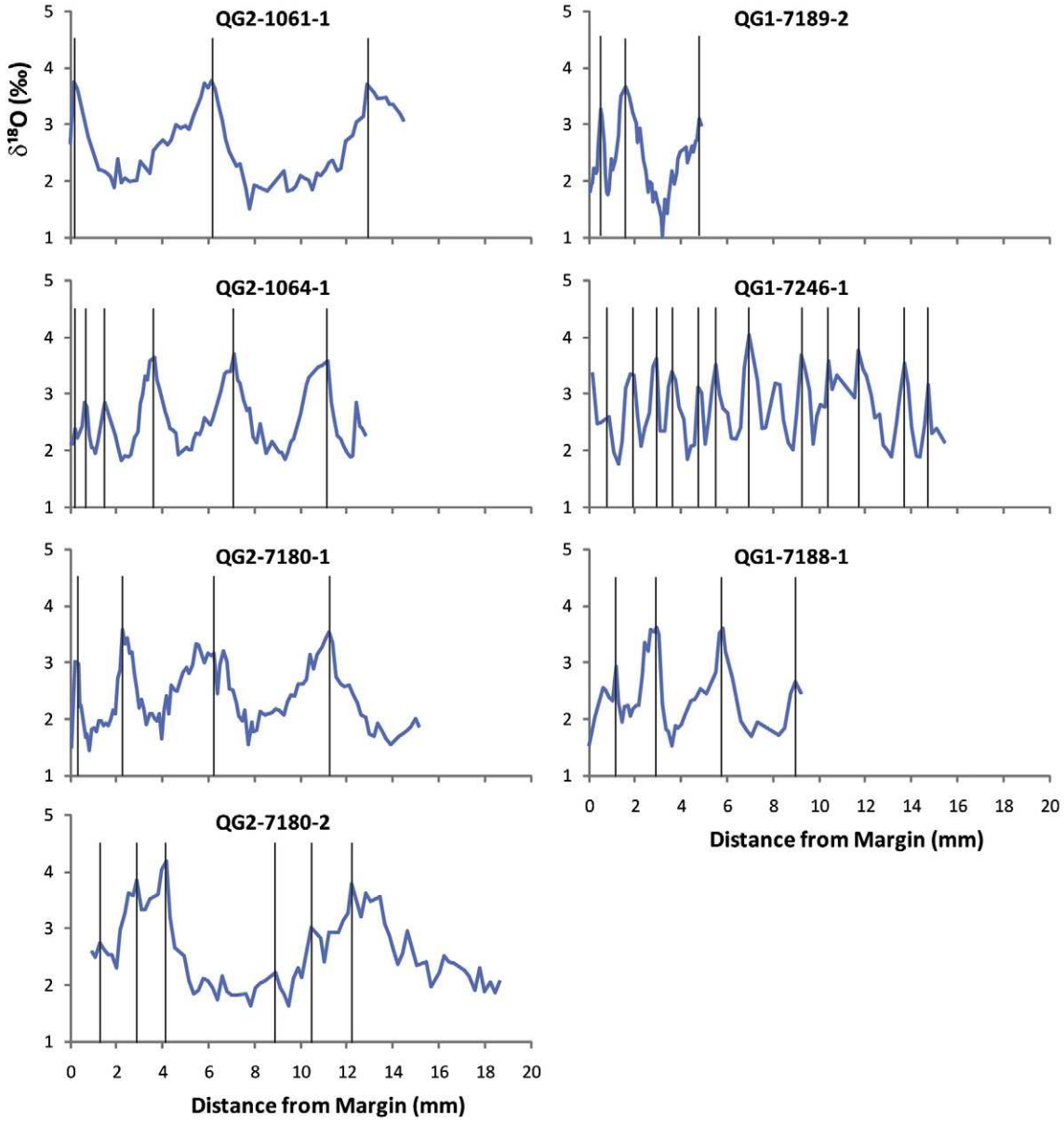


**Fig. 3.** $\delta^{18}O$ values vs. distance from growth margin to apex in mm (growth direction is from right to left) of MCA shells from Phase 1 (10th century; specimens QG1-7189-2, QG1-7246-1, and QG1-7188-1) and Phase 2 (11th–12th centuries; specimens QG2-1061-1, QG2-1064-1, QG2-7180-1, and QG2-7180-2). Vertical bars identify locations of prominent growth lines.

not correspond to a concomitant drop in salinity and does not significantly change the mean value if removed.

### 4.2. Oxygen isotope ratios of shell carbonate

All shells have a temporal variation of $\delta^{18}O$ values following a quasi-sinusoidal trend (Fig. 3). With the exception of specimen QG1-7246-1, the time series exhibits a pattern of cuspate peaks (high $\delta^{18}O$ values) and broad valleys (low $\delta^{18}O$ values). Specimen QG1-7246-1 has cuspate peaks and valleys. Prominent growth lines in all shells correspond with peaks; however, one peak in specimen QG1-7246-1 contains no obvious growth line (located at 8.1 mm from the growth margin), and specimen QG2-7180-2 has extra growth lines not associated with peaks (located at 1.3, 2.9, 8.9, and 10.5 mm from the growth margin). Distances between prominent growth lines ranged from around 1 mm (e.g., specimen QG1-7246-1) to 6 mm (e.g., specimen QG2-1061-1) with most increments between growth lines measuring several mm.

## 5. Discussion

### 5.1. Estimated SST and comparison to the late 20th century

The quasi-sinusoidal $\delta^{18}O$ time series of MCA shells from the 10th to 12th centuries all reflect seasonal temperature fluctuation. Like other *Patella* shells from the cold-temperate biogeographic province, prominent growth lines form in the winter (Fenger et al., 2007 and references therein; Wang et al., 2012) (Figs. 3 and 4). A single exception, specimen QG2-7180-2, also formed growth lines during spring (located at 1.3, 2.9 and 10.5 mm from the growth margin) and summer (located at 8.9 mm from the growth margin). These "non-annual" growth lines probably reflect disturbance conditions and are not related to cold-temperature growth cessation.

Averages and ranges of estimated SST are based on $\delta^{18}O$ values and sclerochronologic assessment. Evaluating estimated seasonal averages and ranges of SST in a sclerochronologic context is essential to account for potential time-averaging biases. For example, during times of slowed growth represented by cusps in the oxygen isotope time series,

**Table 2**
Oxygen isotope ratios of surface water collected from the bay, Rack Wick, near Quoygrew on Westray, Orkney.

| Date | Salinity (psu) | Measured $\delta^{18}O_{WATER}$ (‰ VSMOW) | Estimated[a] $\delta^{18}O_{WATER}$ (‰ VSMOW) |
|---|---|---|---|
| 2 Aug 2005 | 34 | 0.13 | 0.12 |
| 1 Sept 2005 | 34 | 0.24 | 0.12 |
| 1 Oct 2005 | 35 | 0.29 | 0.30 |
| 1 Nov 2005 | 35 | −0.12 | 0.30 |
| 1 Jan 2006 | 35 | 0.39 | 0.30 |
| 4 Feb 2006 | 35 | 0.39 | 0.30 |
| 1 Mar 2006 | 34.5 | 0.43 | 0.21 |
| 1 Apr 2006 | 35.5 | 0.45 | 0.39 |
| 1 May 2006 | 34.5 | 0.40 | 0.21 |
| 1 July 2006 | 35.5 | 0.44 | 0.39 |
| 24 Aug 2006 | 35 | 0.33 | 0.30 |
| Average | 34.8 | 0.31 | 0.27 |
| Standard deviation | 0.5 | 0.17 | 0.09 |

[a] Estimated using Eq. (1) in Austin and Inall (2002).

more time is averaged than during periods of fast growth characterized by broad valleys in the time series. Thus, temperature estimated at cusps in the $\delta^{18}O$ time series may not capture the lowest winter or highest summer temperature, whereas the likelihood of capturing the actual seasonal temperature during fast growth (broad valleys in this case) is greatest. Table 3 presents the maximum and minimum temperatures measured at the peaks and valleys of all the specimens (Fig. 4). We flagged estimated temperatures with potential time-averaging biases and average annual growth increments less than 1 mm/year due to slowed growth with ontogeny (increasing age) or irregular growth rates due to environmental stress.

After culling SST with potential time-averaging biases, the coldest winter SST recorded in all specimens ranged from 4.0 °C to 7.9 °C and averaged 6.0 ± 0.6 °C (i.e., values in brackets in Table 3). Interannual winter variability was relatively stable as recorded in all shells. Two especially cold winters were recorded in specimens QG1-7246-1 (4.5 °C; 10th century) and QG2-7180-2 (4.0 °C; 11th–12th centuries). The warmest summer SST ranged from 13.0 °C to 16.9 °C and averaged 14.1 ± 0.7 °C. In this case, we excluded specimen QG1-7246-1 from our summer SST estimates because of the potentially truncated records at cuspate summer portions of the time series compared to the more broad summer portions exhibited in the other specimens. Removing this shell from our summer SST estimates does not significantly affect the overall mean or our conclusions. If included, the mean and standard deviation is 13.9 ± 0.9 °C. As in winter, interannual summer variability was relatively constant. The resultant seasonal range from the 10th to 12th centuries was ~8 °C.

MCA shells were compared to monthly records of modern SST near the study area for years 1961 to 1990 obtained from the temperature record centered at 60°N, 2°W around a 1° grid (i.e., 59.5–60.5°N, 1.5-2.5°W) from the National Oceanic and Atmospheric Administration (NOAA) Extended Reconstructed SST V2 database (http://www.ncdc.noaa.gov/ersst/) (Fig. 5). The average modern SST for the coldest month is 7.77 ± 0.40 °C and the warmest month is 12.42 ± 0.41 °C. Based on the NOAA data set, modern SST has a seasonal range of 4.65 °C. The modern gridded SST data are slightly north and west of our study area; however, we do not expect this to affect our conclusions. Wang et al. (2012) reported modern SST (1961–1990) from western Scotland (a 1° grid centered around 56°N, 6°W) where winter and summer SST averaged 7.40 ± 0.35 °C and 14.12 ± 0.54 °C, respectively. A difference of 4° latitude does not significantly influence winter SST between these locations, and summer SST differs by less than 2 °C. Therefore, the slightly northern location of the NOAA SST data relative to our study area has a negligible effect on winter SST and at most results in cooler summer SST by only 0.28 °C, which is within error. Relative to the late 20th century, the MCA shell record indicated that the coldest winter SSTs during the 10th to 12th centuries were ~2 °C colder and the warmest SSTs were ~2 °C warmer. The seasonal amplitude in SST fluctuation during the 10th to 12th centuries (~8 °C) was higher than the late 20th century.

To illustrate the advantages of using archives of SST from fast-growing, short-lived mollusc shells, we compare averages of the shell time series (representing annual averages weighted toward the fast-growing summer season) to the average of the 1961–1990 SST time series in Fig. 5. Averaging MCA shell data yields an overall estimated SST of 10.7 ± 2.4 °C. Average SST for the late 20th century is 9.82 ± 1.66 °C. Without the benefit of seasonal-scale resolution, we would conclude that the early MCA was warmer than the late 20th century by ~1 °C. This conclusion is generally true for the summer season, but not true for the winter season.

### 5.2. Comparison with other studies

We compared our results with paleoclimate studies based on documentary and proxy data and those that reconstruct winter and summer seasons, seasonal amplitude, and annual averages. Ogilvie and Farmer (1997) and Pfister et al. (1998) used documentary evidence to characterize European winter air temperature during the MCA. Cooler winters in our study relative to the late 20th century generally agrees with cold episodes identified in the 11th and 12th centuries in both earlier studies. Pfister et al. (1998) document relatively few "Great Winters" (compared to the Little Ice Age) that punctuate the record between 1100 and 1300 AD, but also report that winters from 1090 to 1179 AD were as cold as those in the LIA. Winters became warmer than the early 20th century (1901–1960) from 1180 to 1209 AD. This characterization agrees with Lamb (1965) whose index of winter mildness/severity in England (Fig. 2 in his paper) indicates more frequent severe winters in the early 12th century and increasingly mild winters in the late 12th, 13th, and 14th centuries. Ogilvie and Farmer (1997) noted that more than a dozen severe and frosty winters occurred in England between c. 1200 and 1439 AD. Several of these winters were sufficiently cold to freeze the Thames, allowing people to cross it on foot. Stable winters in our study are consistent with Pfister et al. (1998), who also noted that several winters were close to 20th century temperatures. Their documentary evidence suggests these "warm phases" lasted for several decades and were possibly linked to changes in thermohaline circulation. This explanation is probably not the case here because the "warm" winters identified in our study are single years, not decade-long runs of milder temperatures. Mangini et al. (2005) used proxy data from a $\delta^{18}O$ stalagmite record to reconstruct winter temperature in the central Alps over the last 2000 years. The rationale of their findings is based on: (1) the temperature control on the $\delta^{18}O$ of precipitation (heavier summer and lighter winter precipitation); and (2) the observation that their temperature estimates (based on stalagmite $\delta^{18}O$ values) corresponded better to the multiproxy winter (DJF) temperature reconstruction of Luterbacher et al. (2004) than to yearly average temperature in the Alps. They conclude that winter temperature during the MCA (800 to 1000 AD) was higher than the average over their 2000 year record and ~1.7 °C on average higher than during the LIA. However, it is difficult to compare our findings to their study because they compared their MCA winter temperature reconstructions with their 2000 yr data set rather than with the late 20th century observational data. In a more recent study, Büntgen et al. (2011) reconstructed a 2500-year record of summer precipitation and winter temperature variability for central Europe based on tree-ring proxy data. Cold winter temperature during the late 10th to early 12th centuries with respect to the period 1901–2000 is in agreement with our findings.

Our observation that warmest summer temperatures recorded in *P. vulgata* shells reflects higher temperatures than the late 20th century is consistent with several studies. Cage and Austin (2010) reconstructed summer bottom water temperature from a core collected from Loch Sunart, which is a fjord basin near our study site in northwest Scotland. Oxygen isotope ratios from benthic foraminifera were interpreted to

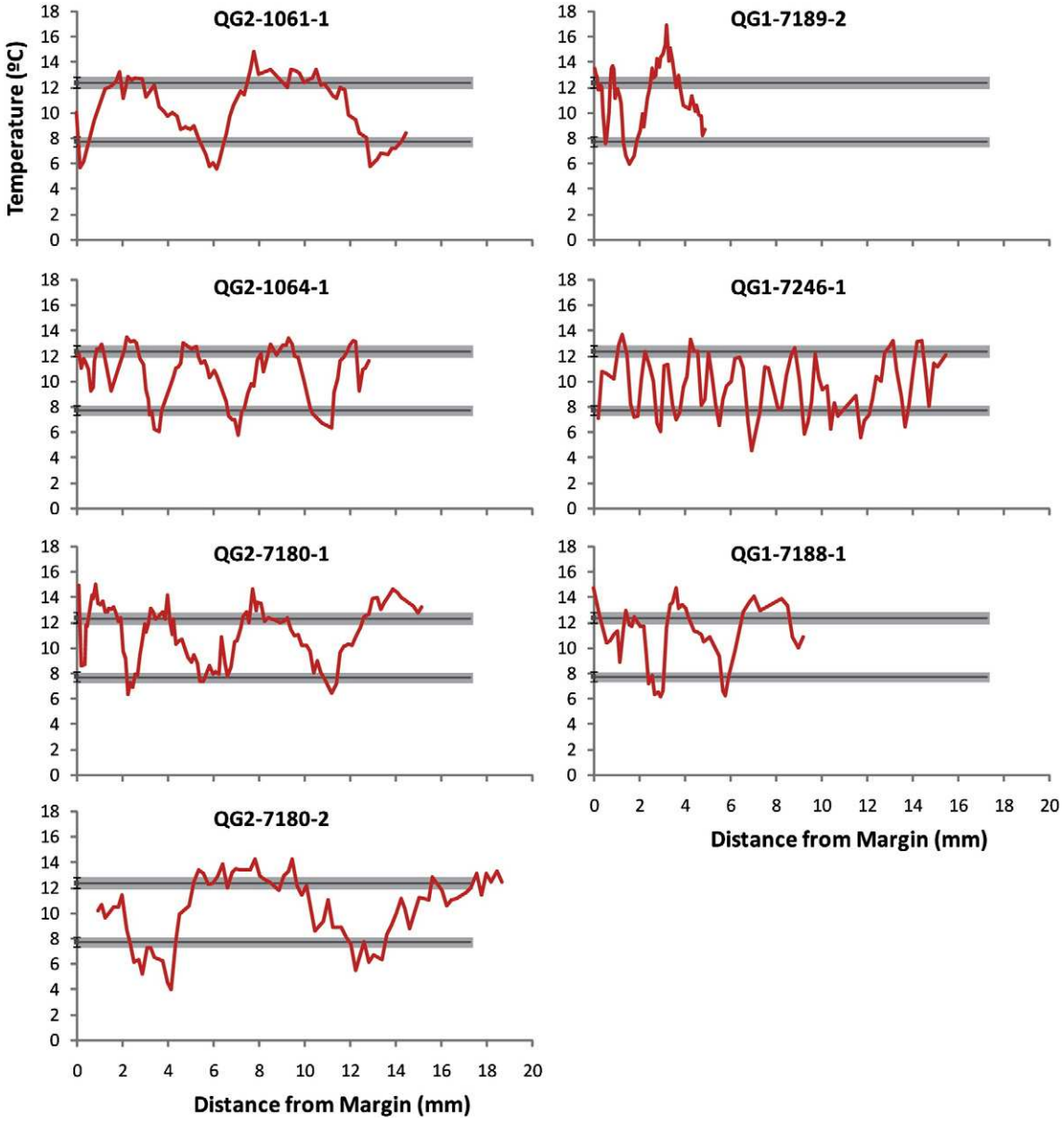


**Fig. 4.** Estimated SSTs from MCA limpets vs. distance from growth margin to apex in mm (growth direction is from right to left) of MCA shells from Phase 1 (10th century; specimens QG1-7189-2, QG1-7246-1, and QG1-7188-1) and Phase 2 (11th–12th centuries; specimens QG2-1061-1, QG2-1064-1, QG2-7180-1, and QG2-7180-2). Horizontal bars indicate the average range of winter SST data (7.77 ± 0.40 °C) and summer SST data (12.42 ± 0.41 °C) from 1960 to 1991 around the grid (60°N, 2°W) provided by the National Oceanic and Atmospheric Administration (NOAA) Extended Reconstructed SST V2 database (http://www.ncdc.noaa.gov/ersst/).

record summer temperature. Although only briefly discussed, summer temperature during the early MCA (10th to 11th centuries) was as warm or warmer than the late 20th century, in agreement with our observations. Warm summers from the Orkney shells are also consistent with studies elsewhere in the North Atlantic. Sicre et al. (2008) reconstructed summer SST from a marine core collected off of northern Iceland over the last 2000 years using alkenone paleothermometry ($U^{K'}_{37}$). A prolonged warm interval during the summer season is observed during the period coinciding with the MCA and is similar to or warmer than modern temperature calculated from water column alkenone data collected during the cruise. On the western side of the North Atlantic, Cronin et al. (2003) reconstructed late Holocene spring temperatures from Mg/Ca paleothermometry using ostracode valves from Chesapeake Bay. Although not synchronous with our study, the early MCA in their time series was relatively warm.

Two recent studies provide seasonally resolved seawater temperature in the North Atlantic based on oxygen isotope paleothermometry of bivalve shells. Patterson et al. (2010) reconstructed a ~2000-year record of 2–9 year snapshots of summer and winter seawater temperature using high-resolution $\delta^{18}O$ values from several species of bivalve shells collected from near-shore marine cores in northwest Iceland. Their data are presented as a summary of maximum and minimum temperatures (i.e., the single warmest and coldest temperatures per shell without associated standard deviations). An oxygen isotope time series for only one of their shell specimens was shown. They report that summer temperature ~960 AD remained relatively high and winter temperature was colder compared to the initial wave of settlement, in agreement with our data for the 10th century. By ~990 AD, they infer that summer temperatures began to decrease, which agrees with Icelandic historical documentation. This pattern was not observed in our shell data. Their isotopic data suggest a warming trend occurred between ~1120 and 1250 AD. Further comparison between our studies is hindered because it is difficult to fully evaluate their temperature reconstructions and conclusions in the absence of standard deviations and without examining the oxygen isotope time series of each shell to assess

**Table 3**
Summary statistics for sea surface temperature (SST) estimated from limpet shells.

| Specimen no. | Distance from margin (mm) | Coldest winter SST (°C) | Warmest summer SST (°C) | Average winter SST with standard deviations (°C) | Average summer SST with standard deviations (°C) | Seasonal SST range (°C) |
|---|---|---|---|---|---|---|
| QG1-7189-2 | 0.1 | | 13.5[a] | 6.8 ± 1 | 14.7 ± 1.9 | 7.9 |
| | 0.5 | 7.6[a] | | [6.0][b] | [15.3 ± 2.3][b] | [9.3][b] |
| | 0.8 | | 13.7 | | | |
| | 1.6 | 6.0 | | | | |
| | 3.21 | | 16.9 | | | |
| QG1-7246-1 | 0.2 | 7.1[a] | | 6.7 ± 1.0 | 12.1 ± 1.3 | 5.4 |
| | 1.3 | | 13.7 | [6.4 ± 1.0][b] | [12.3 ± 0.9][b] | [5.9][b] |
| | 1.8 | 7.2 | | | | |
| | 2.3 | | 12.4[a] | | | |
| | 2.9 | 6.1[a] | | | | |
| | 3.1 | | 11.3 | | | |
| | 3.6 | 7.0 | | | | |
| | 4.3 | | 13.4[a] | | | |
| | 4.7 | 8.2[a] | | | | |
| | 5.0 | | 12.2 | | | |
| | 5.5 | 6.6 | | | | |
| | 6.2 | | 11.8 | | | |
| | 6.9 | 4.5 | | | | |
| | 7.5 | | 11.1 | | | |
| | 8.1 | 7.9 | | | | |
| | 8.8 | | 12.7[a] | | | |
| | 9.2 | 5.9 | | | | |
| | 9.7 | | 12.2 | | | |
| | 10.4 | 6.3 | | | | |
| | 11.5 | | 8.9[a] | | | |
| | 11.7 | 5.6 | | | | |
| | 13.0 | | 12.7 | | | |
| | 13.7 | 6.5 | | | | |
| | 14.4 | | 13.2 | | | |
| | 14.7 | 8.0[a] | | | | |
| QG1-7188-1 | 0.0 | | 14.7[a] | 7.1 ± 1.6 | 14.1 ± 0.8 | 7.0 |
| | 1.2 | 8.9[a] | | [6.2 ± 0.1][b] | [13.9 ± 0.9][b] | [7.8][b] |
| | 1.4 | | 13.0 | | | |
| | 2.9 | 6.1 | | | | |
| | 3.6 | | 14.7 | | | |
| | 5.8 | 6.2 | | | | |
| | 7.1 | | 14.1 | | | |
| QG2-1061-1 | 0.1 | 5.7 | | 5.7 ± 0.1 | 14.1 ± 1.1 | 8.4 |
| | 1.9 | | 13.3 | | | |
| | 6.1 | 5.6 | | | | |
| | 7.8 | | 14.9 | | | |
| | 12.9 | 5.8 | | | | |
| QG2-1064-1 | 0 | 9.2a | 12.4[a] | 7.3 ± 1.8 | 13.1 ± 0.4 | 5.8 |
| | 0.6 | | | [6.1 ± 0.3][b] | [13.2 ± 0.2][b] | [7.2][b] |
| | 1.1 | 9.3[a] | 13.0 | | | |
| | 1.5 | | | | | |
| | 2.2 | 6.1 | 13.5 | | | |
| | 3.6 | | | | | |
| | 4.7 | 5.8 | 13.1 | | | |
| | 7.1 | | | | | |
| | 9.3 | 6.3 | 13.4 | | | |
| | 11.2 | | | | | |
| | 12.1 | | 13.2 | | | |
| QG2-7180-1 | 0.1 | | 14.9[a] | 7.2 ± 1.1 | 14.7 ± 0.3 | 7.5 |
| | 0.3 | 8.7[a] | | [6.7 ± 0.6][b] | | [7.7][b] |
| | 0.8 | | 15.0 | | | |
| | 2.3 | 6.3 | | | | |
| | 4.0 | | 14.2 | | | |
| | 5.6 | 7.4 | | | | |
| | 7.7 | | 14.6 | | | |
| | 11.2 | 6.5 | | | | |
| | 13.9 | | 14.7 | | | |
| QG2-7180-2 | 4.2 | 4.0 | | 4.8 ± 1.1 | 13.8 ± 0.7 | 9.0 |
| | 7.8 | | 14.3 | | | |
| | 12.2 | 5.5 | | | | |
| | 18.4 | | 13.3 | | | |

[a] Flagged annual growth increments <1 mm (i.e., slowed growth with ontogeny or due to environmental stress).
[b] Values in brackets are calculated after removing flagged temperatures.

potential time-averaging biases. In a more recent study, Wanamaker et al. (2011) used subannually resolved $\delta^{18}O$ values of subfossil bivalve shells (*Arctica islandica*) from the northwestern Atlantic (Gulf of Maine, USA) to reconstruct past seasonal changes in seawater temperature during the MCA and LIA. Their results are opposite to our findings. *A. islandica* shells from their study recorded decreased seasonality

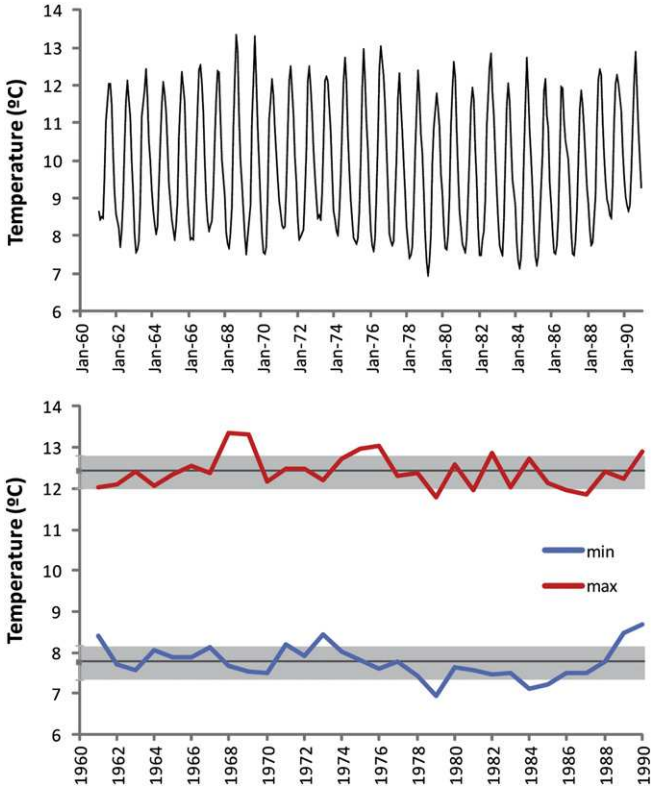


**Fig. 5.** SST for the period 1960–1991 around the grid (60°N, 2°W) provided by the National Oceanic and Atmospheric Administration (NOAA) Extended Reconstructed SST V2 database (http://www.ncdc.noaa.gov/ersst/). Top panel is monthly time series. Bottom panel is warmest summer SST (red line), coldest winter SST (blue line), and summer (12.42 ± 0.41 °C) and winter (7.77 ± 0.40 °C) mean/standard deviation (horizontal bars).

during the 11th century compared to the late 20th century, whereas SST archives from our study reflect increased seasonality. In contrast to our study, the shells from the Gulf of Maine reflected colder summers and warmer winters compared to summers and winters in the 14th and late 19th centuries (LIA). They explained the inferred decreased seasonality during medieval times as a likely result of increased stratification of coastal waters due to warmer seawater temperatures. The contrasting findings between these two studies may result from differences in regional hydrography: stratification in the Gulf of Maine vs. well-mixed coastal waters near Orkney.

Several studies report on SST during the MCA reconstructed from proxy records with annual to decadal resolution. Keigwin (1996) found warm SST during the MCA based on $\delta^{18}O$ values of the planktonic foraminifera, *Globigerinoides ruber*, from the Sargasso Sea. *G. ruber* lives year round; therefore, the temperature estimates are annual averages and not easily compared to our seasonal-scale findings. Our times series are biased towards the summer season when growth rates of shell carbonate are fastest. Hence, weighted averages of annual increments reflect warmer conditions during the MCA, which is not accurate based on our seasonally resolved data. Nevertheless, increased summer SST in our study is consistent with the findings of Keigwin (1996), but cold winter temperature recorded in MCA shells is not. Closer to our study area, McDermott et al. (2001) reconstructed a centennial-scale record of Holocene climate variability based on speleothem $\delta^{18}O$ values from southwestern Ireland. They noted the approximate timing of historical climate episodes, such as the MCA, in their time series, but did not focus their discussion on these intervals. It is difficult to draw conclusions or make comparisons with this study because, as with other speleothem records, $\delta^{18}O$ values may be influenced by changes in moisture source and/or storm track trajectories; thus, temperature changes cannot be estimated precisely.

### 5.3. Possible climate mechanisms

The MCA was the most recent warm episode of European climate prior to industrialization, yet its spatial and temporal character is not well understood. Also uncertain are the driving mechanisms influencing climate during the MCA and LIA. Trouet et al. (2009) presented a nearly 1000-year long multidecadal NAO reconstruction based on proxy data from a tree-ring record from Morocco and a speleothem record from Scotland. The tree ring data from Morocco records February-to-June Palmer Drought Severity Index, and the speleothem record reflects winter precipitation for Scotland. Both locations represent the southern and northern nodes of the NAO dipole, respectively. The records were normalized over the common period 1049–1995 AD. They identified persistent positive NAO conditions during the MCA from ~1100 AD to the early 1400 s. The NAO reconstruction shifted toward weaker conditions during the LIA. The persistent positive NAO conditions from their study occur later than the early MCA records from our study. They further suggest that the persistent positive NAO conditions during the MCA were probably coupled to La Niña-like conditions in the equatorial Pacific amplified by an intensified Atlantic meridional overturning circulation (AMOC) during the MCA. Lund et al. (2006) reconstructed Gulf Stream density structure and transport during the last millennium, supporting an intensification of meridional overturning circulation and oceanic heat transport in the North Atlantic. In agreement with Trouet et al. (2009), Mann et al. (2009) presented decadal SST reconstructions synthesizing multiproxy data sets of the entire Northern Hemisphere (NH) mean, Atlantic Multidecadal Oscillation (AMO), Pacific Decadal Oscillation and the Niño3 sector of the equatorial Pacific. The period from ~950 to 1100 AD shows the highest temperature anomalies in the NH mean and AMO, and cooler temperature anomalies in the earlier part of the record from ~900 to 950 AD. Recently, Wanamaker et al. (2012) reconstructed changes in North Atlantic surface ocean circulation and climate based on the local radiocarbon reservoir age offset (ΔR), a water mass tracer, based on an annually resolved shell chronology from the north Icelandic shelf spanning the last 1350 years. They report that AMOC dynamics likely amplified the relatively warm conditions of the MCA and relatively cool conditions of the LIA in the North Atlantic sector. Trouet et al. (2012) considered an alternative hypothesis that changes in the degree of storminess/cyclogenesis in the North Atlantic influenced the NAO state. However, their study focuses on the MCA/LIA transition, which is much later than the early MCA records in our study. In a more recent study, Lehner et al. (2012) report that results from transient model simulations neither support a persistent positive NAO during the MCA, nor a strong phase shift of the NAO when passing into the LIA. They conclude that results from their study "should motivate both the proxy and model community to work toward a revised assessment of the role of the NAO during the first half of the last millennium."

Our findings are consistent with Mann et al. (2009), although the cool winter conditions are not exactly synchronous with their proxy compilation which covers a much larger area. Colder winters and increased seasonality observed in our study do not fit well with positive NAO conditions. Upon closer inspection, the earliest part of the NAO reconstruction by Trouet et al. (2009) shows low NAO conditions. The speleothem data from Scotland used in their reconstruction extend further back to 900 AD and show low winter NAO conditions in the 11th century. Perhaps our shell data are capturing the lower NAO conditions observed in the speleothem data from Scotland. We will test this hypothesis in the future using radiocarbon-dated shells and seasonally resolved isotopic shell data from high medieval times when other proxy data suggest European climate was warmest and from the subsequent LIA.

## 6. Conclusions

Our study provides reconstructed SST variability at seasonal time scales in the North Atlantic along northern coastal Scotland during the early MCA (10th to 12th centuries). We illustrate the value of using climate archives from fast-growing, short-lived mollusc shells. Such high-resolution archives simultaneously record winter and summer seasons and, unlike more traditional proxy records, approach the full seasonal range of temperature. Because the shells in our study grow fastest during the warm season, the $\delta^{18}O$ time series are weighted toward summer SST. Thus, if we attempt to calculate annual SST by averaging the time series, our annual averages would be biased toward warm temperatures. We would conclude that the early MCA was ~1 °C warmer than the late 20th century. Based on our seasonally resolved time series, this observation is broadly true for summer SST, but not true for winter SST. During their growth period, MCA shells recorded colder winters and warmer summers (by ~2 °C) than the late 20th century. Our findings are consistent with other proxy and documentary data that are restricted to a single season. One study, however, shows opposite results (Wanamaker et al., 2011) perhaps reflecting differences in the regional hydrography. Cold winters and increased seasonality are inconsistent with positive NAO conditions and may represent lower NAO conditions. We will test this hypothesis in the future using: (1) radiocarbon-dated shells from later in the MCA and from the LIA; (2) increased numbers of shells analyzed per phase; and (3) analysis of modern shells for comparison with the isotopic records of the archaeological specimens.

## Acknowledgments

Thanks to David Dettman at the Environmental Isotope Laboratory, University of Arizona, for isotopic analysis of water and carbonate samples, to Mike Mobilia for assisting in shell selection, preparation, and microsampling, to Jennifer Harland for initial processing of the excavated sediment samples, to Nicky Milner for initial identification of the shell taxa, and to the Orkney Museum for access to the archived collection. Gina Rendall and Margaret Drever kindly collected the monthly seawater samples from Rack Wick Bay. Ting Wang illustrated the map figure and determined calibrated radiocarbon ages. We thank two anonymous reviewers for improving the quality of this paper. Funding was provided to DS by the National Geographic Society (Award No. 8214–07) and the National Science Foundation (Award No. AGS-0602422). The main funding for the Quoygrew excavation was provided by grants to JHB from Historic Scotland, The Social Sciences and Humanities Research Council (Canada), the British Academy, Orkney Islands Council and the Society for Medieval Archaeology.

## References

Andrus, C.F.T., 2011. Shell midden sclerochronology. Quaternary Science Reviews 30 (21–22), 2892–2905.
Austin, W.E.N., Inall, M.E., 2002. Deep-water renewal in a Scottish fjord: temperature, salinity and oxygen isotopes. Polar Research 21 (2), 251–257.
Austin, W.E.N., Cage, A.G., Scourse, J.D., 2006. Mid-latitude shelf seas: a NW European perspective on the seasonal dynamics of temperature, salinity and oxygen isotopes. The Holocene 16 (7), 937–947.
Barrett, J.H., 2005. Economic intensification in Viking Age and medieval Orkney, Scotland: excavations at Quoygrew. In: Mortensen, A., Arge, S.V. (Eds.), Viking and Norse North Atlantic: Selected papers from the proceedings of the Fourteenth Viking Congress, Føroya Fróðskaparfela: Annales Societatis Scientiarum Færoensis Supplementum, XLIV, pp. 264–283 (Tórshavn).
Barrett, J.H. (Ed.), in press. Being an Islander: Production and Identity at Quoygrew, Orkney, AD 900–1600. McDonald Institute for Archaeological Research, Cambridge, United Kingdom.
Büntgen, U., Tegel, W., Nicolussi, K., McCormick, M., Frank, D., Trouet, V., Kaplan, J.O., Herzig, F., Heussner, K.-U., Wanner, H., Luterbacher, J., Esper, J., 2011. 2500 years of European climate variability and human susceptibility. Science 331 (6017), 578–582.
Cage, A.G., Austin, W.E.N., 2010. Marine climate variability during the last millennium: the Loch Sunart record, Scotland, UK. Quaternary Science Reviews 29 (13–14), 1633–1647.
Christiansen, B., Ljungqvist, F.C., 2011. Reconstruction of the extratropical NH mean temperature over the last millennium with a method that preserves low-frequency variability. Journal of Climate 24 (23), 6013–6034.
Cohen, A.L., Branch, G.M., 1992. Environmentally controlled variation in the structure and mineralogy of *Patella granularis* shells from the coast of southern Africa: implications for palaeotemperature assessments. Palaeogeography, Palaeoclimatology, Palaeoecology 91, 49–57.
Connor, D.W., Gilliland, P.M., Golding, N., Robinson, P., Todd, D., Verling, E., 2006. UKSeaMap: the mapping of seabed and water column features of UK seas. Joint Nature Conservation Committee, Peterborough.
Coplen, T.B., Kendall, C., Hopple, J., 1983. Comparison of stable isotope reference samples. Nature 302 (5905), 236–238.
Cronin, T.M., Dwyer, G.S., Kamiya, T., Schwede, S., Willard, D.A., 2003. Medieval Warm Period, Little Ice Age and 20th century temperature variability from Chesapeake Bay. Global and Planetary Change 36, 17–29.
Diaz, H.F., Trigo, R., Hughes, M.K., Mann, M.E., Xoplaki, E., Barriopedro, D., 2011. Spatial and temporal characteristics of climate in Medieval times revisited. Bulletin of the American Meteorological Society 92 (11), 1487–1500.
Fenger, T., Surge, D., Schöne, B., Milner, N., 2007. Sclerochronology and geochemical variation in limpet shells (*Patella vulgata*): a new archive to reconstruct coastal sea surface temperature. Geochemistry, Geophysics, Geosystems 8 (7), Q07001. http://dx.doi.org/10.1029/2006gc001488.
Ferguson, J.E., Henderson, G.M., Fa, D.A., Finlayson, J.C., Charnley, N.R., 2011. Increased seasonality in the Western Mediterranean during the last glacial from limpet shell geochemistry. Earth and Planetary Science Letters 308 (3–4), 325–333.
Friedman, I., O'Neil, J.R., 1977. Compilation of stable isotope fractionation factors of geochemical interest. In: Fleischer, M. (Ed.), Data of Geochemistry. United States Government Printing Office, Washington, DC, pp. KK1–KK12.
Gonfiantini, R., Stichler, W., Rozanski, K., 1995. Standards and intercomparison materials distributed by the International Atomic Energy Agency for stable isotope measurements. Reference and intercomparison materials for stable isotopes of light elements. I.A.E.A, pp. 13–29.
Graham, N., Ammann, C., Fleitmann, D., Cobb, K., Luterbacher, J., 2011. Support for global climate reorganization during the "Medieval Climate Anomaly". Climate Dynamics 37 (5), 1217–1245.
Hallmann, N., Burchell, M., Schöne, B.R., Irvine, G.V., Maxwell, D., 2009. High-resolution sclerochronological analysis of the bivalve mollusk *Saxidomus gigantea* from Alaska and British Columbia: techniques for revealing environmental archives and archaeological seasonality. Journal of Archaeological Science 36 (10), 2353–2364.
Helama, S., Hood, B.C., 2011. Stone Age midden deposition assessed by bivalve sclerochronology and radiocarbon wiggle-matching of *Arctica islandica* shell increments. Journal of Archaeological Science 38 (2), 452–460.
Holliday, N.P., 2003. Air-sea interaction and circulation changes in the northeast Atlantic. Journal of Geophysical Research-Oceans 108 (C8).
Hufthammer, A.K., Høie, H., Folkvord, A., Geffen, A.J., Andersson, C., Ninnemann, U.S., 2010. Seasonality of human site occupation based on stable oxygen isotope ratios of cod otoliths. Journal of Archaeological Science 37 (1), 78–83.
Hughen, K.A., Baillie, M.G.L., Bard, E., Beck, J.W., Bertrand, C.J.H., Blackwell, P.G., Buck, C.E., Burr, G.S., Cutler, K.B., Damon, P.E., Edwards, R.L., Fairbanks, R.G., Friedrich, M., Guilderson, T.P., Kromer, B., McCormac, G., Manning, S., Ramsey, C.B., Reimer, P.J., Reimer, R.W., Remmele, S., Southon, J.R., Stuiver, M., Talamo, S., Taylor, F.W., van der Plicht, J., Weyhenmeyer, C.E., 2004. Marine04 marine radiocarbon age calibration, 0–26 cal kyr BP. Radiocarbon 46, 1059–1086.
Huthnance, J.M., 1992. Extensive slope currents and the ocean-shelf boundary. Progress in Oceanography 29 (2), 161–196.
Huthnance, J.M., 1995. Circulation, exchange and water masses at the ocean margin: the role of physical processes at the shelf edge. Progress in Oceanography 35 (4), 353–431.
Inall, M., Gillibrand, P., Griffiths, C., MacDougal, N., Blackwell, K., 2009. On the oceanographic variability of the North-West European Shelf to the West of Scotland. Journal of Marine Systems 77 (3), 210–226.
Jansen, E., Overpeck, J., Briffa, K.R., Duplessy, J.-C., Joos, F., Masson-Delmotte, V., Olago, D., Otto-Bliesner, B., Peltier, W.R., Rahmstorf, S., Ramesh, R., Raynaud, D., Rind, D., Solomina, O., Villalba, R., Zhang, D., 2007. Palaeoclimate. In: Solomon, S., et al. (Ed.), Climate Change 2007: The Physical Science Basis. Contribution of Working Group I to the Fourth Assessment Report of the Intergovernmental Panel on Climate Change. Cambridge University Press, Cambridge, United Kingdom and New York, NY, USA, pp. 433–497.
Jones, K.B., Hodgins, G.W.L., Etayo-Cadavid, M.F., Andrus, C.F.T., Sandweiss, D.H., 2010. Centuries of marine radiocarbon reservoir age variation with archaeological *Mesodesma donacium* shells from southern Peru. Radiocarbon 52 (3), 1207–1214.
Keigwin, L.D., 1996. The Little Ice Age and Medieval Warm Period in the Sargasso Sea. Science 274, 1504–1508.
Lamb, H.H., 1965. The early Medieval warm epoch and its sequel. Palaeogeography, Palaeoclimatology, Palaeoecology 1, 13–37.
Lee, S., Kim, H.-K., 2003. The dynamical relationship between subtropical and eddy-driven jets. Journal of the Atmospheric Sciences 60 (12), 1490.
Lehner, F., Raible, C.C., Stocker, T.F., 2012. Testing the robustness of a precipitation proxy-based North Atlantic Oscillation reconstruction. Quaternary Science Reviews 45, 85–94.
Lund, D.C., Lynch-Stieglitz, J., Curry, W.B., 2006. Gulf Stream density structure and transport during the past millennium. Nature 444 (7119), 601–604.
Luterbacher, J., Dietrich, D., Xoplaki, E., Grosjean, M., Wanner, H., 2004. European seasonal and annual temperature variability, trends, and extremes since 1500. Science 303 (5663), 1499–1503.
Mangini, A., Spötl, C., Verdes, P., 2005. Reconstruction of temperature in the Central Alps during the past 2000 yr from a $\delta^{18}O$ stalagmite record. Earth and Planetary Science Letters 235 (3–4), 741–751.

Mann, M.E., Zhang, Z., Rutherford, S., Bradley, R.S., Hughes, M.K., Shindell, D., Ammann, C., Faluvegi, G., Ni, Fenbiao, 2009. Global signatures and dynamical origins of the Little Ice Age and Medieval Climate Anomaly. Science 326 (5957), 1256–1260.

McDermott, F., Mattey, D.P., Hawkesworth, C., 2001. Centennial-scale Holocene climate variability revealed by a high-resolution speleothem $\delta^{18}O$ record from SW Ireland. Science 294, 1328–1331.

Milner, N., Barrett, J., Welsh, J., 2007. Marine resource intensification in Viking Age Europe: the molluscan evidence from Quoygrew, Orkney. Journal of Archaeological Science 34, 1461–1472.

Ogilvie, A.E.J., Farmer, G., 1997. Documenting the Medieval Climate. In: Hulme, M., Barrow, E. (Eds.), Climates of the British Isles. Present, Past and Future. Routledge, London, pp. 112–133.

Owen, R., Kennedy, H., Richardson, C., 2002. Isotopic partitioning between scallop shell calcite and seawater: effect of shell growth rate. Geochimica et Cosmochimica Acta 66 (10), 1727–1737.

Patterson, W.P., Dietrich, K.A., Holmden, C., Andrews, J.T., 2010. Two millennia of North Atlantic seasonality and implications for Norse colonies. Proceedings of the National Academy of Sciences of the United States of America 107 (12), 5306–5310.

Pfister, C., Schwarz-Zanetti, G., Wegmann, M., Luterbacher, J., 1998. Winter air temperature variations in western Europe during the Early and High Middle Ages (AD 750–1300). The Holocene 8 (5), 535–552.

Reimer, P.J., Baillie, M.G.L., Bard, E., Bayliss, A., Beck, J.W., Blackwell, P.G., Ramsey, C.B., Buck, C.E., Burr, G.S., Edwards, R.L., Friedrich, M., Grootes, P.M., Guilderson, T.P., Hajdas, I., Heaton, T.J., Hogg, A.G., Hughen, K.A., Kaiser, K.F., Kromer, B., McCormac, F.G., Manning, S.W., Reimer, R.W., Richards, D.A., Southon, J.R., Talamo, S., Turney, C.S.M., van der Plicht, J., Weyhenmeye, C.E., 2009. INTCAL09 and MARINE09 radiocarbon age calibration curves, 0–50,000 years cal BP. Radiocarbon 51, 1111–1150.

Russell, N., Cook, G.T., Ascough, P., Barrett, J.H., Dugmore, A., 2011. Species specific marine radiocarbon reservoir effect: a comparison of ΔR values between *Patella vulgata* (limpet) shell carbonate and *Gadus morhua* (Atlantic cod) bone collagen. Journal of Archaeological Science 38, 1008–1015.

Scourse, J.D., Kennedy, H., Scott, G.A., Austin, W.E.N., 2004. Stable isotopic analyses of modern benthic foraminifera from seasonally stratified shelf seas: disequilibria and the 'seasonal effect'. The Holocene 14 (5), 747–758.

Shackleton, N.J., 1973. Oxygen isotope analysis as a means of determining season of occupation of prehistoric midden sites. Archaeometry 15 (1), 133–141.

Sicre, M.-A., et al., 2008. Decadal variability of sea surface temperatures off North Iceland over the last 2000 years. Earth and Planetary Science Letters 268 (1–2), 137–142.

Simpson, I.A., Barrett, J.H., Milek, K.B., 2005. Interpreting the Viking Age to medieval period transition in Norse Orkney through cultural soil and sediment analyses. Geoarchaeology 20, 355–388.

Souza, A.J., Simpson, J.H., Harikrishnan, M., Malarkey, J., 2001. Flow structure and seasonality in the Hebridean slope current. Oceanologica Acta 24, S63–S76.

Stuiver, M., Reimer, P.J., Reimer, R.W., 2005. CALIB Radiocarbon Calibration. http://radiocarbon.pa.qub.ac.uk/calib2005.

Surge, D., Walker, K.J., 2005. Oxygen isotope composition of modern and archaeological otoliths from the estuarine hardhead catfish (*Ariopsis felis*) and their potential to record low-latitude climate change. Palaeogeography, Palaeoclimatology, Palaeoecology 228 (1–2), 179–191.

Tarutani, T., Clayton, R.N., Mayeda, T.K., 1969. The effect of polymorphism and magnesium substitution on oxygen isotope fractionation between calcium carbonate and water. Geochimica et Cosmochimica Acta 33, 987–996.

Trouet, V., Esper, J., Graham, N.E., Baker, A., Scourse, J.D., Frank, D.C., 2009. Persistent positive North Atlantic Oscillation mode dominated the Medieval Climate Anomaly. Science 324 (5923), 78–80.

Trouet, V., Scourse, J.D., Raible, C.C., 2012. North Atlantic storminess and Atlantic Meridional Overturning Circulation during the last Millennium: reconciling contradictory proxy records of NAO variability. Global and Planetary Change 84–85, 48–55.

van der Schrier, G., Drijfhout, S.S., Hazeleger, W., Noulin, L., 2007. Increasing the Atlantic subtropical jet cools the circum-North Atlantic. Meteorologische Zeitschrift 16 (6).

Walker, K.J., Surge, D., 2006. Developing oxygen isotope proxies from archaeological sources for the study of Late Holocene human–climate interactions in coastal southwest Florida. Quaternary International 150 (1), 3–11 (Special Issue: Impact of rapid environmental changes on humans and ecosystems).

Wanamaker, A.D., Kreutz, K.J., Schone, B.R., Introne, D.S., 2011. Gulf of Maine shells reveal changes in seawater temperature seasonality during the Medieval Climate Anomaly and the Little Ice Age. Palaeogeography, Palaeoclimatology, Palaeoecology 302 (1–2), 43–51.

Wanamaker, A.D., Butler, P.G., Scourse, J.D., Heinemeier, J., Eiríksson, J., Knudsen, K.L., Richardson, C.A., 2012. Surface changes in the North Atlantic meridional overturning circulation during the last millennium. Nature Communications 3, 899.

Wang, T., Surge, D., Walker, K.J., 2011. Isotopic evidence for climate change during the Vandal Minimum from *Ariopsis felis* otoliths and *Mercenaria campechiensis* shells, southwest Florida, USA. The Holocene 21 (7), 1081–1091.

Wang, T., Surge, D., Mithen, S., 2012. Seasonal temperature variability of the Neoglacial (3300–2500 BP) and Roman Warm Period (2500–1600 BP) reconstructed from oxygen isotope ratios of limpet shells (*Patella vulgata*), Northwest Scotland. Palaeogeography, Palaeoclimatology, Palaeoecology 317–318, 104–113.